JOC Article

Experimental and Computational Studies of Selective Recognition of Hg^{2+} by Amide Linked Lower Rim 1,3-Dibenzimidazole Derivative of Calix[4]arene: Species Characterization in Solution and that in the Isolated Complex, Including the Delineation of the Nanostructures

Roymon Joseph, Balaji Ramanujam, Amitabha Acharya, Anupam Khutia, and Chebrolu P. Rao*

Department of Chemistry Indian Institute of Technology Bombay, Powai, Mumbai 400076, India

cprao@iitb.ac.in

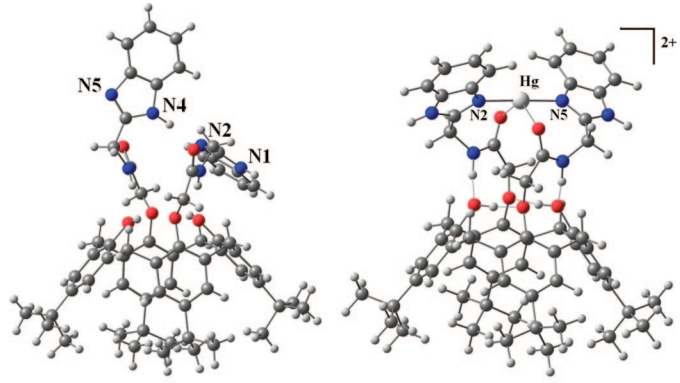

L $L+Hg^{2+}$

Amide linked lower rim 1,3-dibenzimidazole derivative of calix[4]arene, L has been shown to be sensitive and selective to Hg^{2+} in aqueous acetonitrile solution based on fluorescence spectroscopy, and the stoichiometry of the complexed species has been found to be 1:1. The selectivity of L toward Hg^{2+} has been shown among 11 M^{2+} ions, viz., Mn^{2+}, Fe^{2+}, Co^{2+}, Ni^{2+}, Cu^{2+}, Zn^{2+}, Cd^{2+}, Hg^{2+}, Pb^{2+}, Ca^{2+}, and Mg^{2+} studied, including those of the mercury group and none of these ions impede the recognition of Hg^{2+} by L. Role of the solvent on the recognition of Hg^{2+} has been demonstrated. The role of calix[4]arene platform and the benzimidazole moieties in the recognition of Hg^{2+} by L has been delineated upon performing such studies with five different molecules of relevance as reference molecular systems. The binding cores formed by the receptor L and the reference compounds have been established based on the single crystal XRD structures, and the preferential metal ion binding cores have been discussed. The binding of Hg^{2+} with L has been further established based on ^{1}H and ^{13}C NMR, ESI MS, absorption, and fluorescence lifetime measurements. Some of these techniques have been used to establish the stoichiometry of the species formed. The complex species formed between L and Hg^{2+} have been isolated and characterized and found to be 1:1 species even in the isolated complex. Whereas transmission electron microscopy (TEM), atomic force microscopy (AFM), and scanning electron microscopy (SEM) provided the nanostructural behavior of L, the TEM and SEM demonstrated that the mercury complex has different characteristics when compared to L. The TEM, SEM, and powder XRD studies revealed that whereas L is crystalline, that of the mercury complex is not, perhaps a reason for not being able to obtain single crystals of the complex. Binding characteristics of Hg^{2+} toward L have been established based on the DFT computational calculations.

Introduction

Supramolecular systems like calixarenes[1] functionalized with suitable metal ion binding cores can act as good hosts for the recognition of metal ions.[2] Among these the well studied were those based on calix[4]arene. However, the calix[4]arene based molecular systems were rather scarce in the literature in detecting toxic, nonradioactive as well as volatile heavy metallic element, such as, mercury.[3] Though there are several other molecular systems for sensing Hg^{2+}, calix[4]arene based ones are scarce in the literature and include upper rim functionalized with aryl-azo group[4] and lower rim calix[4]aza-crown derivatives possessing different fluorescent probes including those of dansyl groups.[5] These are generally studied in various organic

* To whom correspondence should be addressed. Phone: 91 22 2576 7162. Fax: 91 22 2572 3480.

10.1021/jo800073g CCC: $40.75 © 2008 American Chemical Society
Published on Web 07/01/2008

SCHEME 1. Synthesis of the Receptor Molecule, L[a]

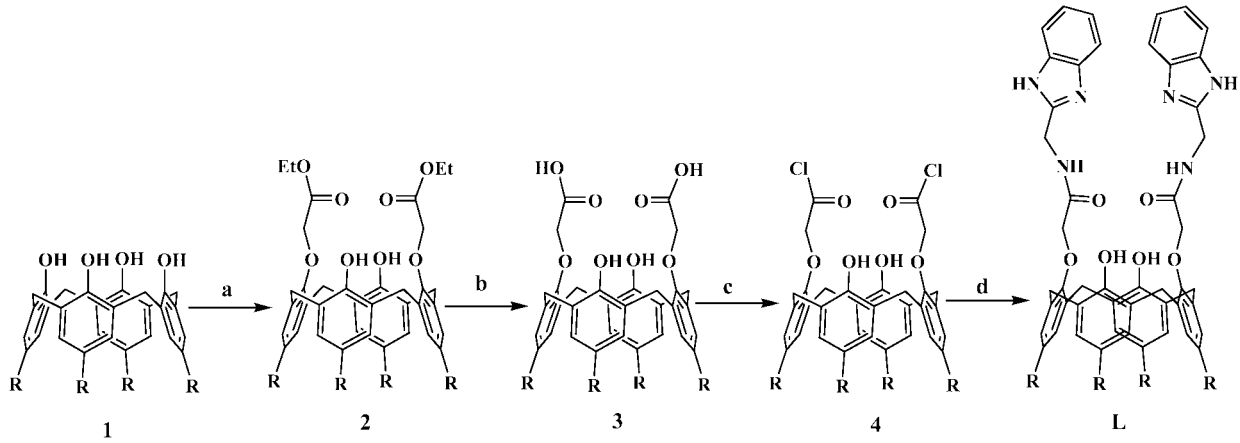

[a] Synthesis of lower rim calix[4]arene-1,3-diderivatives, L: (a) bromoethylacetate/K_2CO_3/ acetone; (b) NaOH/C_2H_5OH, reflux; (c) $SOCl_2$/benzene, reflux; (d) 2-aminomethylbenzimidazole/Et_3N/THF. R = tert-butyl.

solvents and those studied in aqueous medium were limited. Therefore, the development of molecular systems that can selectively recognize Hg^{2+} continues to intrigue researchers. In this regard, we report the development of a biologically relevant benzimidazole attached lower rim 1,3-diderivative of calix[4]arene (L), connected through amide links for the purpose of selectively recognizing Hg^{2+} in aqueous solution. The data has been compared with that of the judiciously selected reference molecules. The binding cores of the receptor and reference molecules have been established by structure determination. The present studies include the delineation of all its properties suitable for selective recognition of Hg^{2+} in aqueous solution, and also the isolation and characterization of the species formed. Nanostructural difference between the L and its mercury complex has been demonstrated. The nature of the mercury complex has been addressed by DFT computational calculations.

Results and Discussion

The selective recognition of Hg^{2+} by the receptor molecule, L in aqueous solution has been demonstrated primarily using fluorescence spectroscopy and has been further supported by other techniques, such as, absorption, NMR, and ESI MS. The selectiveness of L has been convincingly demonstrated upon comparing the data obtained from similar studies carried out with appropriately chosen reference molecular systems.

Receptor Molecule (L). The receptor molecule, L, has been synthesized in four known steps[6] (Scheme 1). The reaction of **1** with bromoethylacetate results in the formation of 1,3-diester derivative, **2**, and its hydrolysis yielded the corresponding diacid derivative, **3**. The diacid, **3**, when treated with $SOCl_2$ resulted in the formation of diacid chloride, **4**, and this upon coupling with 2-aminomethylbenzimidazole resulted in the receptor molecule, L. All the compounds exhibited satisfactory analytical and spectral data as given in the Experimental section.

Reference Molecules (L_1, L_2, L_3, L_4, and L_5). The reference compounds, L_1, L_2, L_3, L_4, and L_5 (Figure 1) have been selected keeping in mind the importance or necessity of different chemical units present in L including that of the calixarene platform. Therefore, this resulted in choosing the molecules, such as, simple 2-aminomethyl benzimidazole (L_1) without having the calixarene platform, calix-amide without possessing benzimidazole moieties (L_2), pyridyl derivative (L_3) that could mimic the benzimidazole unit only in part as far as the nitrogen coordination center is concerned, calix-amide derivative possessing only the hydrophobic moiety (L_4) but not the coordination centers and the benzimidazole derivative of only p-tert-butylphenol without having the total calixarene framework (L_5). Whereas L_1 was purchased, L_2, L_3, and L_4 were synthesized by reacting **4** with the appropriate amine moiety, viz., dibenzylamine, 2-aminomethylpyridine and methyl ester of phenylalanine respectively to result in L_2, L_3, and L_4. L_5 has been synthesized starting from *p*-tert-butyl-phenol followed by ester,

(1) (a) Gutsche, C. D. *Calixarenes*; Royal Society of Chemistry: Cambridge, U.K., 1989. (b) Rao, C. P.; Dey, M. *Encycl. Nanosci. Nanotech.* **2004**, *1*, 475.
(2) (a) Lee, Y. O.; Choi, Y. H.; Kim, J. S. *Bull. Korean Chem. Soc.* **2007**, *28*, 1–151. (b) Quang, D. T,; Jung, H. S.; Yoon, J. H.; Lee, S. Y; Kim, J. S. *Bull. Korean Chem. Soc.* **2007**, *28*, 682. (c) Dalbavie, J.-O.; Regnouf-de-Vains, J.-B; Lamartine, R.; Perrin, M.; Lecocq, S.; Fenet, B. *Eur. J. Inorg. Chem.* **2002**, 901. (d) Belhamel, K.; Nguyen, T. K. D.; Benamor, M.; Ludwig, R. *Eur. J. Inorg. Chem.* **2003**, 4110. (e) Kim, S. K.; Kim, S. H.; Kim, H. J.; Lee, S. H.; Lee, S. W.; Ko, J.; Bartsch, R. A.; Kim, J. S. *Inorg. Chem.* **2005**, *44*, 7866. (f) Lee, S. H.; Kim, J. Y.; Ko, J.; Lee, J. Y.; Kim, J. S. *J. Org. Chem.* **2004**, *69*, 2902. (g) Kim, S. K.; Lee, S. H.; Lee, J. Y.; Lee, J. Y.; Bartsch, R. A.; Kim, J. S. *J. Am. Chem. Soc.* **2004**, *126*, 16499. (h) Kim, J. S.; Shon, O. J.; Rim, J. A.; Kim, S. K.; Yoon, J. *J. Org. Chem.* **2002**, *67*, 2348. (i) Kim, J. S.; Noh, K. H.; Lee, S. H.; Kim, S. K.; Kim, S. K.; Yoon, J. *J. Org. Chem.* **2003**, *68*, 597. (j) Lee, J. Y.; Kim, S. K.; Jung, J. H.; Kim, J. S. *J. Org. Chem.* **2005**, *70*, 1463. (k) Choi, J. K.; Kim, S. H.; Yoon, J.; Lee, K.-H.; Bartsch, R. A.; Kim, J. S *J. Org. Chem.* **2006**, *71*, 8011. (l) Kim, J. S.; Kim, H. J.; Kim, H. M.; Kim, S. H.; Lee, J. W.; Kim, S. K.; Cho, B. R. *J. Org. Chem.* **2006**, *71*, 8016. (m) Liang, Zhi.; Liub, Z.; Gao, Y *Tetrahedron Lett.* **2007**, *48*, 3587. (n) Banthia, S.; Samanta, A. *Org. Biomol. Chem.* **2005**, *3*, 1428. (o) Chang, K.-C.; Su, I.-H; Senthilvelan, A.; Chung, W.-S. *Org. Lett.* **2007**, *9*, 3363. (p) Ozturk, G.; Akkaya, E. U. *Org. Lett.* **2004**, *6*, 241. (q) Bu, J.-H.; Zheng, Q.-Y.; Chen, C.-F.; Huang, Z.-T *Org. Lett.* **2004**, *6*, 3301. (r) Cao, Y.-D.; Zheng, Q.-Y.; Chen, C.-F.; Huang, Z.-T *Tetrahedron Lett.* **2003**, *44*, 4751. (s) Saiki, T.; Iwabuchi, J.; Akine, S.; Nabeshima, T. *Tetrahedron Lett.* **2004**, *45*, 7007. (t) Kim, S. H.; Choi, J. K.; Kim, S. K.; Simb, W.; Kim, J. S. *Tetrahedron Lett.* **2006**, *47*, 3737. (u) Praveen, L.; Ganga, V. B.; Thirumalai, R.; Sreeja, T.; Reddy, M. L. P.; Varma, R. L. *Inorg. Chem.* **2007**, *46*, 6277. (v) Kim, J. S.; Quang, D. T. *Chem. Rev.* **2007**, *107*, 3780.
(3) (a) Renzoni, A.; Zino, F.; Franchi, E. *Environ. Res.* **1998**, *77*, 68. (b) Boening, D. W. *Chemosphere* **2000**, *40*, 1335.
(4) (a) Kao, T.-L.; Wang, C.-C.; Pan, Y.-T.; Shiao, Y.-J.; Yen, J.-Y.; Shu, C.-M.; Lee, G.-H.; Peng, S.-M.; Chung, W.-S. *J. Org. Chem.* **2005**, *70*, 2912. (b) Ho, I.-T.; Lee, G.-H.; Chung, W.-S. *J. Org. Chem.* **2007**, *72*, 2434.
(5) (a) Talanova, G. G.; Elkarim, N. S. A.; Talanov, V. S.; Bartsch, R. A. *Anal. Chem.* **1999**, *71*, 3106. (b) Choi, M. J.; Kim, M. Y.; Kim, J. R.; Chang, S.-K. *Chem. Lett.* **2000**, 1432. (c) Choi, M. J.; Kim, M. Y.; Chang, S.-K. *Chem. Commun.* **2001**, 1664. (d) Cha, N. R.; Kim, M. Y.; Kim, Y. H.; Choe, J.-I.; Chang, S.-K. *J. Chem. Soc., Perkin Trans.* **2002**, *2*, 1193. (e) Kim, J. H.; Hwang, A.-R.; Chang, S.-K. *Tetrahedron Lett.* **2004**, *45*, 7557. (f) Chen, Q.-Y.; Chen, C.-F. *Tetrahedron Lett.* **2005**, *46*, 165. (g) Me′tivier, R.; Leray, I.; Lebeau, B.; Valeur, B. *J. Mater. Chem.* **2005**, *15*, 2965. (h) Me′tivier, R.; Leray, I.; Valeur, B. *Chem.−Eur. J.* **2004**, *10*, 4480.
(6) Collins, E. M.; McKervey, M. A.; Madigan, E.; Moran, M. B.; Owens, M.; Ferguson, G.; Harris, S. J. *J. Chem. Soc., Perkin Trans. 1* **1991**, 3137.

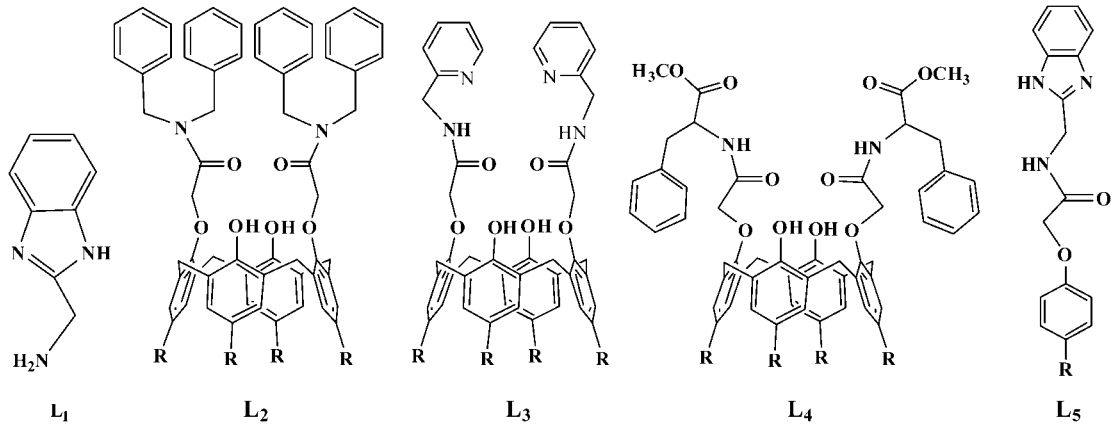

L₁ **L₂** **L₃** **L₄** **L₅**

FIGURE 1. Schematic structures of reference compounds, L_1, L_2, L_3, L_4, and L_5. R = tert-butyl.

TABLE 1. Crystallographic Parameters for the Structure Determination and Refinement[a]

	L_2	L_4	L
Empirical Formula	$C_{76}H_{86}N_2O_6 \cdot 2(CHCl_3)$	$2(C_{68}H_{82}N_2O_{10}) \cdot H_2O$	$C_{64}H_{74}N_6O_6 \cdot 3(C_2H_5OH)$
Temperature (K)	293	120	150
Crystal System	Triclinic	Monoclinic	Triclinic
Space group	$P\bar{1}$ (No. 2)	$P2_1$ (No. 4)	$P\bar{1}$ (No. 2)
a/Å	10.164(5)	14.4663(4)	13.1060(14)
b/Å	16.251(5)	26.1325(7)	13.467(4)
c/Å	23.654(5)	17.0631(5)	21.4629(19)
α/°	97.756(5)	90	76.369(16)
β/°	99.898(5)	96.133(3)	74.335(9)
γ/°	96.042(5)	90	73.248(16)
Volume/Å^3	3781(2)	6413.6(3)	3441.1(12)
Z	2	2	2
Reflections collected	17477	66808	34518
Independent reflections	10676	22341	11985
R_{int}	0.037	0.103	0.042
Reflections used[b]	6350	13689	6118
Parameters	873	1478	797
Final *R*	0.0736	0.0863	0.0710
R′[c]	0.2255	0.1814	0.2260

[a] Structure of L_3 has been reported by us earlier (ref 7). [b] = $[I > 2.0\ \sigma(I)]$ [c] = $1/[s^2(F_o^2) + (0.1133P)^2 + 1.8869P]$ where $P = (F_o^2 + 2F_c^2)/3$.

then acid and its coupling to give the amide derivative of benzimidazole. All these derivatives were characterized by NMR, FTIR, and mass spectroscopy as given in the Experimental section. The ^{1}H NMR data for the receptor and reference compounds clearly suggested cone-conformation for calix[4]arene moiety in case of these derivatives and were further confirmed based on single crystal X-ray structure determinations. The role of calix[4]arene platform in conjunction with the benzimidazole core in the selective recognition of Hg^{2+} by L has been demonstrated in this paper by comparing the results obtained in case of L with those obtained with the reference compounds.

Single Crystal X-Ray Structures of the Reference and Receptor Molecules. Single crystal X-ray structural analysis were carried out in case of L_2, L_3, L_4, and L and the corresponding details of the structure determination and refinement are given in Table 1. All the crystal structures confirmed the formation of 1,3- arms through the amide linkages disposed on the same side of the calix[4]arene at the lower rim to result in binding cores and the nature of the conformation of calix[4]arene was found to be the cone, as has also been demonstrated based on NMR studies (Figure 2).

In all these lower-rim diderivatives, there are two intrarim O−H···O hydrogen bonds present to maintain the cone conformational structure. The conformation of the strands in L_3, L_4, and L are similar up to the amide NH and conformations do change beyond these among the different structures. L_2 cannot show this because the amide group in this case does not have any hydrogen attached to its nitrogen center. The stereoviews and the metric data of all these structures are given in the Supporting Information, S1. The main conformational angles of both the arms are given in Table 2 for L_2, L_3, L_4, and L based on their single crystal XRD structures.

As can be noted from the structure of L_2 (Figure 2a), both the arms exhibited different conformations. One of the arms is more bent than the other as can be judged from the intrastrand O···N distances, viz., 3.009 vs 3.561 Å, and also from the intrastrand O−C−C−N dihedral angle, viz., −71.5 vs −159.6°. As a result of this the N to OH(phenolic) distances are 4.26 to 4.50 Å on the bent side and 5.27 to 5.50 Å on the other side, indicating that the strands are reasonably normal to the lower rim and hence are away from extending any H-bond interaction between the N and phenolic-OH moieties. This may be a result of the absence of hydrogen on amide nitrogen.

In the crystal structure of L_3[7] (Figure 2b), both the strands were bent to almost the same extent as can be judged from the intrastrand O−C−C-N dihedral angles, viz., 12.2 vs 19.6°, so that N−H of the amide groups form hydrogen bond with the lower-rim phenolic −OH groups. The resulting N−H···O hydrogen bonds have N···O distances of 2.955 and 3.027 Å and N−H···O angle of 171.5 and 172.2°. Molecule L_3

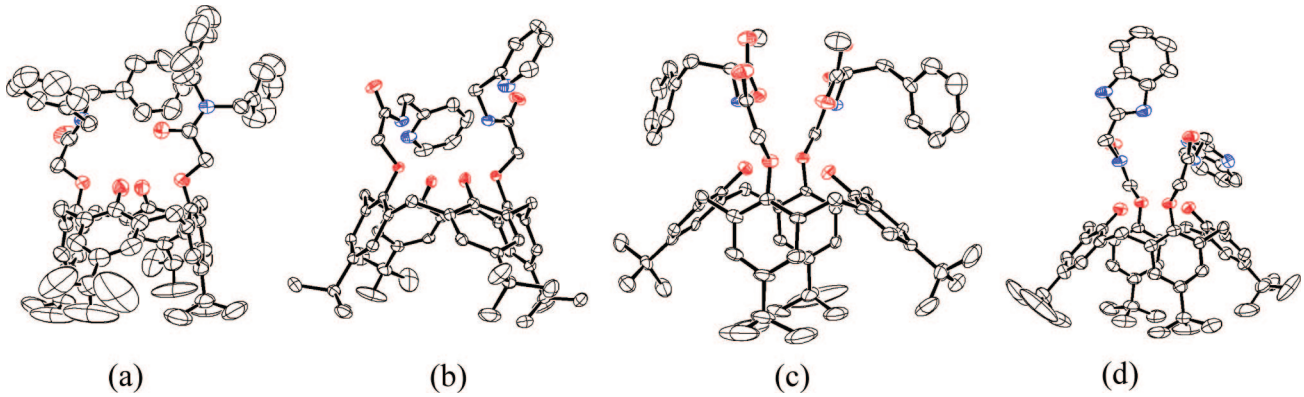

FIGURE 2. ORTEP views of the molecular structures as obtained from their single crystal XRD: (a) L_2; (b) L_3, (c) L_4, and (d) L.

TABLE 2. Selected Dihedral Angles of Both the Arms Based on the Crystal Structures of Receptor and Reference Molecules

dihedral angle[a]	L		L_2		L_3		L_4	
D1	149.0	151.4	−155.5	−172.7	−162.7	−142.7	−149.3	−153.4
D2	−9.2	−21.1	−71.4	−159.6	19.6	12.2	19.9	19.7
D3	−168.5	−169.7	4.3,−174.9	177.0, −10.4	−178.1	173.4	−177.3	−175.2
D4	−62.0	−179.7	−102.9, −105.1	99.0, 111.7	−83.6	−178.3	−84.1, 151.6	−96.0, 141.5

[a] The dihedral angles D1 to D4 are sequential ones starting from the calixarene lower rim carbon. D1 = C_{cal}–O–CH_2–CO; D2 = O–CH_2–CO–N; D3 = CH_2–CO–N–CH_2; D4 = CO–N–C–C.

crystallizes along with a molecule of methanol. The methanol molecule extends a hydrogen bond with the pyridyl nitrogen of one of the arms with a O···N distance of 2.881 Å and O−H···N angle of 173.3° and is also in hydrogen bonding distance with that of the phenolic-OH exhibiting a O···O distance of 3.153 Å. Though both the strands are on the same side, the two strands differ in their C−N−C−C_{py} dihedral angle, viz., −83.6 vs −178.3°, and this results in a large separation between two pyridyl nitrogens, viz., 7.720 Å though the amide nitrogens were disposed close by 3.576 Å, and hence is suited as an N_4 binding core. Therefore, a conformational change is a prerequisite if L_3 should act as tetradentate ligand which can use four nitrogens for binding to metal ions. On the other hand, each of the strand is independently capable of forming a bidentate N_2 binding core to two different metal ions meaning that two different N_2 cores being formed instead of an N_4 core.

In case of L_4, two molecules are present in the asymmetric unit cell where these are related by a pseudo 2-fold axis thereby resulting in a head-to-tail arrangement of these. Both the strands of L_4 exhibit similar dihedral angles indicating similar conformation for both the strands and the same is true for the other molecule too. Even L_4, like that in L_3, both the strands exhibit intramolecular hydrogen bonds between amide N−H and phenolic-OH groups with N···O distances of 3.041 and 2.996 and hydrogen bond angles of 172.8 and 176.9°. As a result of this a N_2O_2 core that is suitable for binding metal ion is being formed using the carbonyl oxygens of the ester moieties. The phenyl moieties are oriented away from the core region. Molecule L_4 can also exhibit an N_2O_6 (Figure 2c) wherein metal ions such as lanthanide may perhaps fit well with some adjustment in the cavity. Thus, there are two possible cores formed in L_4: whereas the N_2O_2 is at the top portion, the N_2O_6 is closer to the lower rim.

In the structure of the receptor molecule, L (Figure 2d), the conformations of the both the strands are different from each other as can be judged from the dihedral angles about C−N−C-C(im) (−179.7 vs −62.1°) and N−C−C(im)-N(H) (−80.1 vs 23.5°). As a result, one of the benzimidazole moieties is aligned along the pseudo 2-fold vertical axis of the calix[4]arene while the other is perpendicular to the axis. Thus while one of the imidazole units is perpendicular to the plane of the lower rim, the other is parallel to it. But the amide N−H in both these is hydrogen bonded to the phenolic O−H groups with N···O distances of 3.050, 3.036 Å and hydrogen bond angle of 163.3 and 169.0°. The two benzimidazole moieties are connected through a strong N−H···N hydrogen bond with N···N distance of 2.863 Å and hydrogen bond angle of 179.8°. This kind of an arrangement results in the formation of N_4 core that can be fitted to a distorted tetrahedron, unlike that observed in case of the pyridyl derivative, L_3. Formation of an N_4 core at the top edge of the calixarene derivative of L is attributed to the presence of two nitrogen centers in the imidazole moiety. At the lower rim, L also exhibits another core of N_2O_4 that can accommodate metal ion. Each L is crystallized along with three ethanol molecules. One of these ethanol units extends a O−H···N hydrogen bond with the imidazole nitrogen of one of the strands where the benzimidazole was parallel to the plane of the lower rim.

Thus among all these structures, it is the L that exhibits an N_4 based core readily at the lower-rim top portion of the molecule, and a some what less accessible core of N_2O_2 is observed with the structure of L_4. All others do not have significant cores that can easily accommodate metal ion, however, L_3 can accommodate metal ion upon some changes in its conformation wherein the two pyridyl nitrogen centers are brought into the inside of the core. These features are evident from the space filling models shown in Figure 3. Of course all the structures have similar hydrophobic cavity.

Thus, in the structures of these free ligands, the ligation centers arising from the arms are not always oriented well in a fashion to bind to the metal ion directly, rather requires some conformational changes before it can bind to a metal ion. Such arrangement may bring preference in the interaction toward one

(7) Rao, P. V.; Rao, C. P.; Kolehmainen, E.; Wegelius, E. K.; Rissanen, K. *Chem. Lett.* **2001**, 1176.

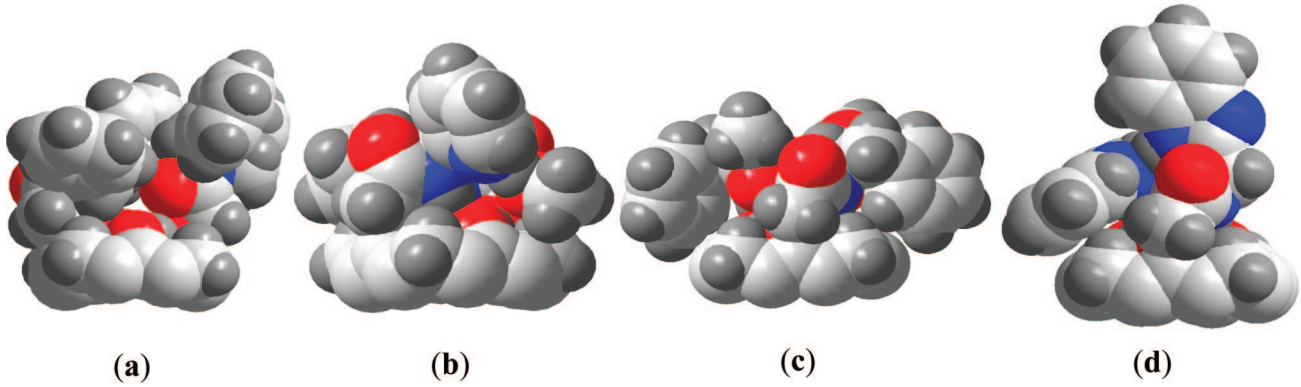

FIGURE 3. Space filling models generated from the corresponding crystal structure data: (a) L_2, (b) L_3, (c) L_4, and (d) L. The arene framework of the calixarene base has been removed for clarity.

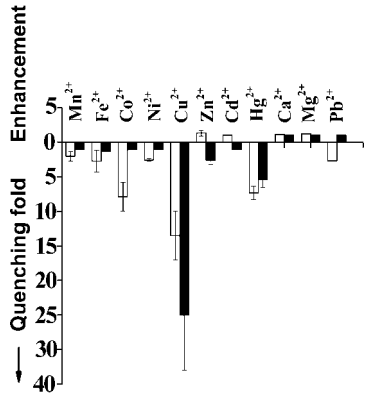

FIGURE 4. Histogram showing the number of times of quenching in the fluorescence intensity in case of titration of L with different M^{2+}. Open columns are for the CH_3CN and the filled columns are for CH_3OH. Error bars were given based on four different measurements.

metal ion over the other and hence these can be explored for their possible selectivity. Results of the corresponding studies are reported in this paper.

Solution Metal Ion Binding Studies. Divalent ions (M^{2+}) such as, Mn^{2+}, Fe^{2+}, Co^{2+}, Ni^{2+}, Cu^{2+}, Zn^{2+}, Cd^{2+}, Hg^{2+}, Pb^{2+}, Ca^{2+}, and Mg^{2+} were studied for their interaction with the molecular systems reported in this paper by fluorescence spectroscopy. Influence of the solvent on such interactions has also been explored. The receptor selectivity of L was discussed in the light of such data obtained with respect to the reference molecules. Further, the species of selective recognition were characterized both in solution as well as in its isolated state including their nanostructural changes and supported the results of titration.

Fluorescence Titration of L with M^{2+} in Organic Solvents. In acetonitrile, when L is excited at 275 nm it exhibits a strong emission maximum around 311 nm. Therefore the fluorescence emission has been used as a handle for studying the interaction of metal ions. The titration of L with M^{2+} in CH_3CN showed fluorescence quenching toward all ions except Zn^{2+}, Ca^{2+} and Mg^{2+}, wherein the quenching follows a trend, viz., $Cu^{2+} \gg Co^{2+} > Hg^{2+} > Mn^{2+} \cong Fe^{2+} \cong Ni^{2+}$ as reported in Figure 4 (Supporting Information, Figure S2). On the other hand, similar titrations carried out in CH_3OH also exhibited quenching with a number of ions and the trend in the fluorescence quenching has been noted to be $Cu^{2+} \gg Hg^{2+} > Zn^{2+} > Fe^{2+}$ as given in Figure 4 (Supporting Information, Figure S2). Though L seems to differentiate metal ions better in CH_3OH than in CH_3CN, there is still no selectivity in any of these solvents toward any one metal ion because either in CH_3OH or in CH_3CN more than one metal ion shows changes in the fluorescence of L. Hence aqueous−organic solutions have been employed for further studies, since such combination is expected to bring changes in the polarity of the medium and the solvation of the metal ion.

Fluorescence Titration of L with M^{2+} in Aqueous Solutions. To change the polarity of the acetonitrile, different volume ratios of water was added to result in water to acetonitrile ratios of 1:3, 1:1 and 3:2, and the fluorescence titrations between L and M^{2+} were carried out in these aqueous solutions. Typical fluorescence spectra obtained during the titration of L with Hg^{2+} in 50% aqueous solution and the corresponding fluorescence intensity ratio plot were given in Figure 5a,b. The extent of fluorescence quenching is defined in terms of the quenching fold and the corresponding results obtained from such titrations performed between the L and M^{2+} in aqueous acetonitrile mixtures were shown in Figure 5c (Supporting Information, Figure S3).

In 50% aqueous solution, a 10-fold quenching was observed only in case of Hg^{2+}, whereas all other M^{2+} exhibited almost no quenching in fluorescence intensity. However, when the content of water was either low (1:3) or high (3:2), the sensitivity of Hg^{2+} detection decreases and a recognizable response is shown even in case of the Cu^{2+}, as a result the selectivity seem to be decreasing at least to some extent (Figure 5c). The species formed between L and Hg^{2+} has been found to be 1:1 based on absorption and ESI MS studies as reported in this paper. Even the Job's plot constructed with the fluorescence data supported the formation of 1:1 complex between Hg^{2+} and L (Supporting Information, Figure S4). Based on the Benesi-Hildebrand equation, the K_{ass} was found to be 20 966 ± 873 M^{-1}. Significant fluorescence intensity changes were observed only in case of the titration of L with Hg^{2+} and not with the other M^{2+} in 1:1 aqueous acetonitrile solution. Hence the 1:1 aqueous solution is well suited for the selective recognition of Hg^{2+} by L. Unlike some of those reported in the literature where a large number of equivalents of Hg^{2+} is required for the formation of 1:1 complex,[5] the present study refers to a stoichiometric titration (Figure 5b). Fluorescence studies performed in 1:1 aqueous solution by varying [Hg^{2+}] but keeping the [Hg^{2+}]/[L] mole ratio at 1:1 indicated a lower limit detection of 1.4 ± 0.1 ppm or less that is accompanied by a decrease in the fluorescence intensity of L by about 10−12% (Supporting Information, Figure S4). Comparison of the fluorescence data obtained among all these different solvent systems clearly

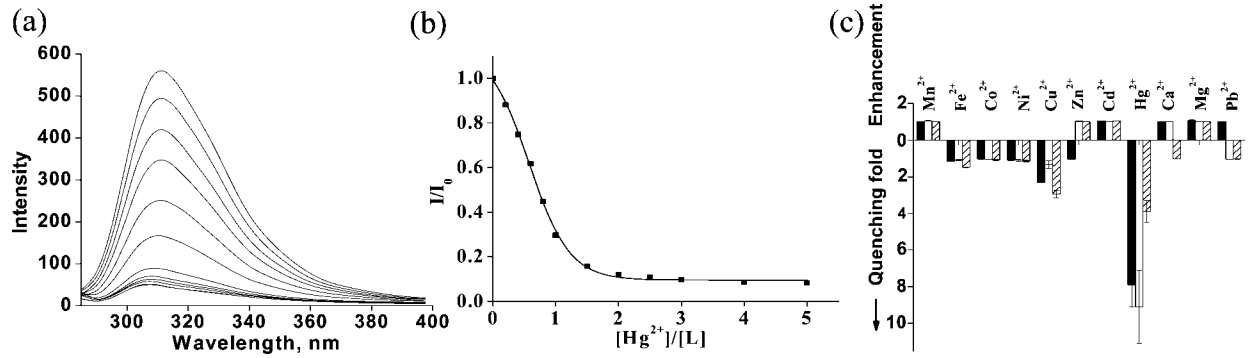

FIGURE 5. (a) Fluorescence spectral traces obtained during the titration of L with Hg^{2+} in 1:1 aqueous acetonitrile. (b) Plot of I/I_0 as a function of $[Hg^{2+}]/[L]$ mole ratio. (c) Histogram showing the number of times of quenching of fluorescence intensity in case of titration of L with different M^{2+} in aqueous acetonitrile solutions. Open columns are for the data in H_2O:CH_3CN of 1:1. Filled columns are for the data in H_2O:CH_3CN of 1:3. Partially filled columns are for the data in H_2O:CH_3CN of 3:2. Error bars were given based on four different measurements.

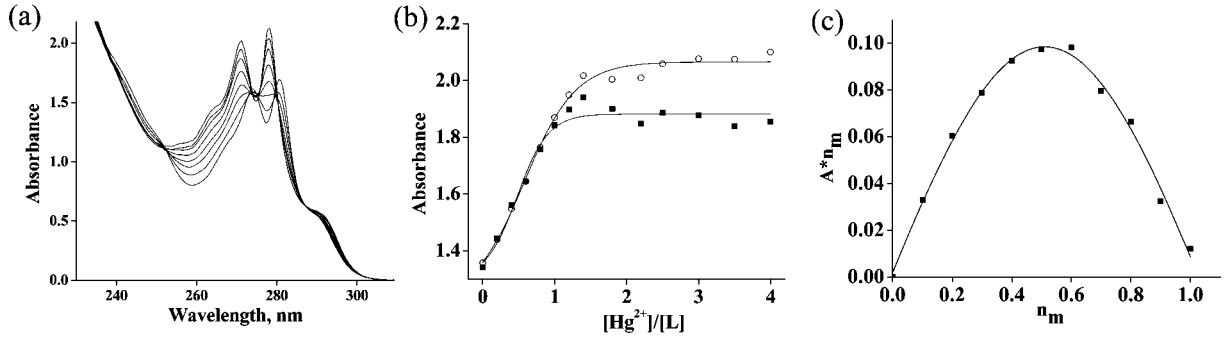

FIGURE 6. Titration of L with Hg^{2+} in 50% aqueous acetonitrile: (a) Absorption spectral traces; (b) Plot of absorbance vs mole ratio of Hg^{2+} added, 271 nm band (○), 277 nm band (■), (c) Job's plot of n_m vs A^*n_m, where n_m is mole fraction of the metal ion added and A is absorbance.

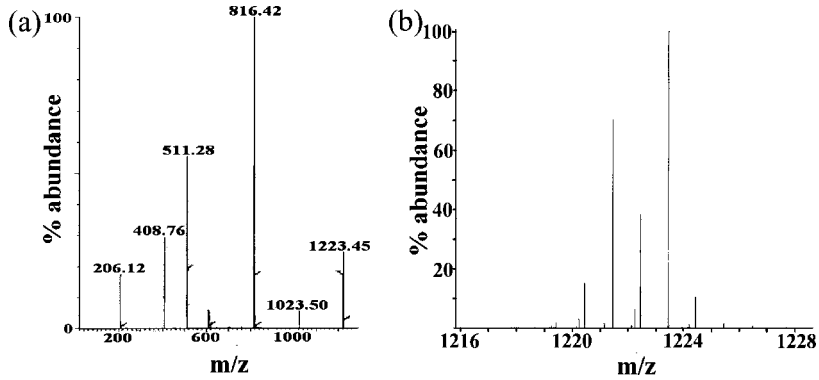

FIGURE 7. (a) ESI mass spectrum showing the molecular ion peak for the 1:1 complex formed between L and Hg^{2+} during titration. (b) Expansion of the molecular ion peak.

suggest that while L retained its sensitivity toward Hg^{2+} in all the aqueous acetonitrile solutions, it is highly selective in 50% aqueous solution implying that L can be a selective receptor for Hg^{2+} in aqueous solution. The binding of Hg^{2+} with L has been further confirmed based on the titrations performed using absorption, ESI MS, and NMR.

Absorption Spectral Studies of L with Hg^{2+}. To confirm the binding of Hg^{2+} with L, absorption spectral studies were carried out for the titration of Hg^{2+} with L in 1:1 aqueous solution. The spectral changes and the isosbestic point observed at 252 and 286 nm in the titration clearly indicate transition between the ligand and the complexed species. Quantitative changes observed in two absorption bands are suggestive of stoichiometric reaction between L and Hg^{2+}. The corresponding Job's plot fits very well with the formation of 1:1 complex (Figure 6).

Electrospray Mass Spectral Studies of L with Hg^{2+}. The complex formed between L and Hg^{2+} has been further confirmed to be 1:1 based on ESI MS. The mass spectra yielded a molecular ion peak for 1:1 complex at m/z of 1223.5, where its isotopic peak pattern supports the presence of Hg^{2+} (Figure 7).

NMR Studies of the Titration of L with Hg^{2+}. During the titration of L with Hg^{2+}, ^1H NMR spectra showed no change in the cone conformation, however, showed marginal to considerable downfield shifts in the δ of C- and N- bound protons of the pendant, amide and benzimidazole moieties to different extents as can be seen from the spectra given in Figure 8. The N−H protons of the benzimidazole showed a downfield shift of ~2.5 ppm and the other benzene protons of the benzimidazole moiety indeed exhibited large downfield shifts. Corresponding metal ion induced shifts for different protons

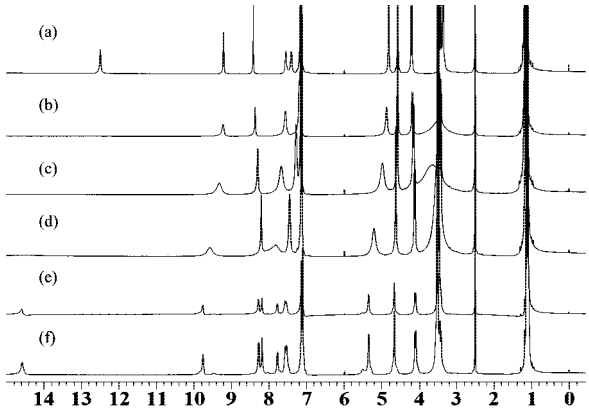

FIGURE 8. ^{1}H NMR spectra measured during the titration of L with Hg^{2+} (in DMSO d6). (a) L, (b) L + 0.25 equiv Hg^{2+}, (c) L + 0.5 equiv Hg^{2+}, (d) L + 1 equiv Hg^{2+}, (e) L + 1.5 equiv Hg^{2+}, (f) L + 2 equiv Hg^{2+}.

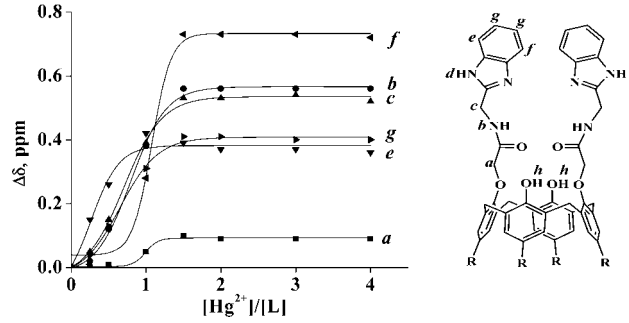

FIGURE 9. Metal ion-induced downfield shifts $\Delta\delta$ ($\Delta\delta = \delta_{(L+Hg^{2+})} - \delta_L$) observed with different protons of L at various mole ratios of $[Hg^{2+}]/[L]$. The labeling for various protons can be seen from the structure given here.

are plotted in Figure 9 and the data indicate that the Hg^{2+} ion mainly interacts with the benzimidazole part of the calix[4]arene derivative. Hg^{2+} induced downfield shifts have also been noticed with the benzimidazole carbons in ^{13}C NMR spectrum (Supporting Information, Figure S5). Such downfield shifts were also noticed in the literature in case of some Hg^{2+} bound complexes.[8] Thus the NMR study clearly supports the binding of Hg^{2+} to benzimidazole moieties in L.

To find whether other metal ions of the mercury group, viz., Zn^{2+} and Cd^{2+}, bind to L or not, absorption titrations were carried out with these ions and found that there are no changes in the absorption spectra of L during the titration with these ions, in aqueous acetonitrile solution (Figure 10). On the other hand, formation of the complex was very clear from the absorption spectra when L was titrated with Hg^{2+} as reported

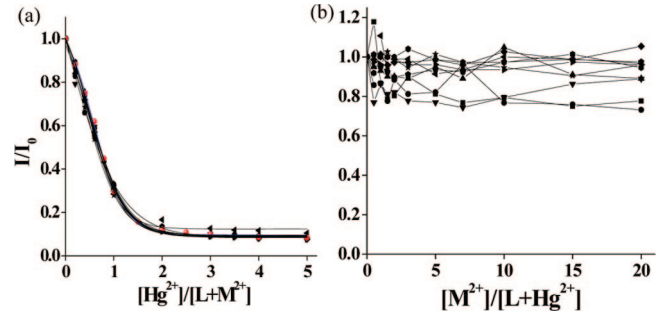

FIGURE 11. Plots of relative fluorescence intensity (I/I_0): (a) Titration of {L + 5*M^{2+}} by Hg^{2+}; (b) Titration of {L + 2*Hg^{2+}} by M^{2+}. The symbols correspond to, ■ = Mn^{2+}; ● = Fe^{2+}; ▲ = Co^{2+}; ▼ = Ni^{2+}; solid triangle pointing left = Cu^{2+}; solid triangle pointing right = Zn^{2+}; ◆ = Cd^{2+}; pentegon = Ca^{2+}; ⬢ = Mg^{2+}; ★ = Pb^{2+}; and red ● = Hg^{2+}.

in this paper. Even the ^{1}H NMR titration carried out between L and Zn^{2+} exhibited only marginal shifts, viz., 0.02 to 0.08 ppm, whereas the shifts are in the range of ~0.1 to 0.8 ppm in case of the titration of L with Hg^{2+}, suggesting that there is no complex formation between L and Zn^{2+} (Supporting Information, Figure S6). Thus all this data clearly support the selective binding of Hg^{2+} even among its group elements (i.e., among Zn^{2+}, Cd^{2+} and Hg^{2+}) to benzimidazole moieties in L.

Competitive Metal Ion Titrations. To establish whether L can selectively recognize Hg^{2+} even in the presence of other metal ions, two types of competitive metal ion titrations were carried out in 1:1 aqueous solution. While in one, it is the Hg^{2+} bound L was titrated with the other M^{2+}, viz., {L + 2*Hg^{2+}} by M^{2+}, in the second case it was the reverse type of titration, viz., {L + 5*M^{2+}} by Hg^{2+}. Such study was expected to reveal the possible use of L in the selective recognition of Hg^{2+}. Based on the two titrations, it is noticed that no M^{2+} has any affect on Hg^{2+} sensing by L as can be seen from the fluorescence intensity ratio plots (Figure 11a and b). Because L has benzimidazole as well as amide moieties, the role of each of these units has also been addressed by extending the titration studies with the reference compounds, viz., L_1, L_2, L_3, L_4, and L_5.

Fluorescence Studies of the Reference Compounds. The fluorescence data obtained with L_1 clearly indicate that more than one M^{2+} quenches the fluorescence and hence is not selective to any M^{2+} (Figure 12a). No change in fluorescence is observed in case of the titration of L_2 with any M^{2+} (Figure 12b), and hence, L_2 is sensitive to any metal ion. Even L_3 does not show any significant changes in the fluorescence by all the M^{2+}, except the Hg^{2+} (Figure 12c), which shows only a partial quenching beyond 10 equivalents and hence does not exhibit much sensitivity toward Hg^{2+}. The L_4 do not show any response

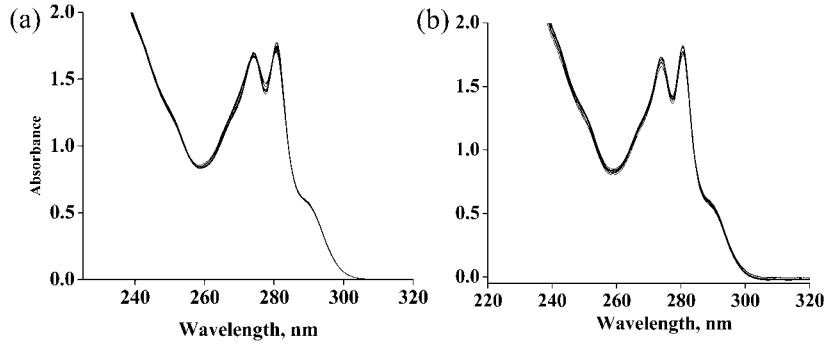

FIGURE 10. Absorption spectra during the titration of L with M^{2+} in 1:1 H_2O:CH_3CN mixture: (a) Zn^{2+} and (b) Cd^{2+}.

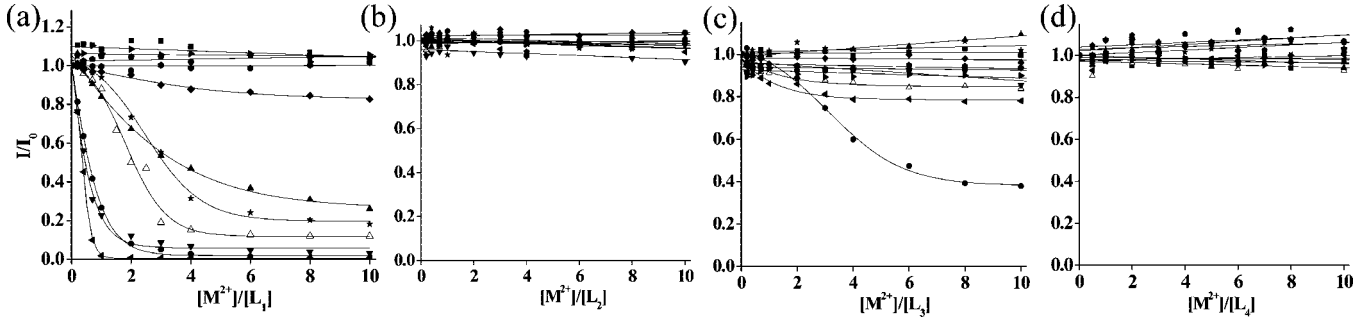

FIGURE 12. Fluorescence titration data for reference compounds in 50% aqueous acetonitrile solution except for (b) which is in 25% aqueous acetonitrile solution: (a) L_1, (b) L_2, (c) L_3, and (d) L_4. The symbols correspond to, ■ = Mn^{2+}; △ = Fe^{2+}; ▲ = Co^{2+};▼ = Ni^{2+}; solid triangle pointing left = Cu^{2+}; solid triangle pointing right = Zn^{2+}; ◆ = Cd^{2+}; pentegon = Ca^{2+}; ⬢ = Mg^{2+}; ★ = Pb^{2+}; and ● = Hg^{2+}.

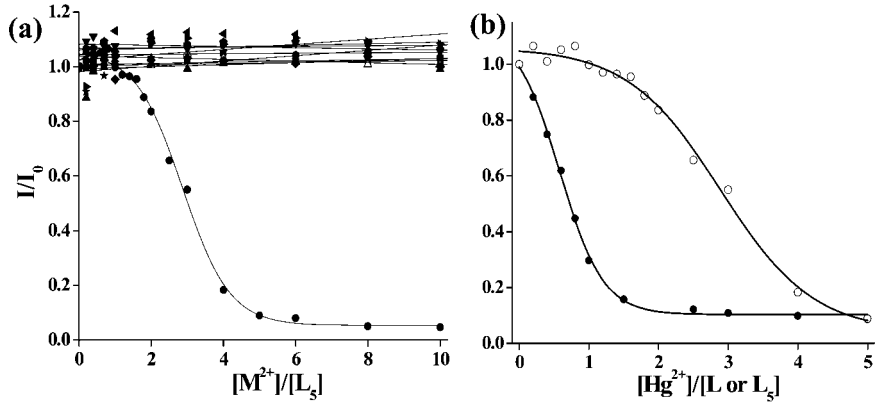

FIGURE 13. Plots of (I/I_0) as a function of metal to the ligand mole ratio during the fluorescence titration studied in aqueous acetonitrile: (a) titration of L_5 with M^{2+} (symbols carry same meaning as those given in Figure 12); (b) titration of L (●) and L_5 (○) with Hg^{2+}.

to M^{2+} including Hg^{2+} (Figure 12d) and hence is neither sensitive nor selective in aqueous solution toward any metal ion. Comparison of the fluorescence titration data of {L + M^{2+}} with that of {L_1 + M^{2+}} clearly suggest that the presence of benzimidazole moiety alone, as in L_1, is not sufficient enough for the recognition of Hg^{2+}. Although L_5 is sensitive only toward Hg^{2+} among all the different M^{2+} studied (Figure 13a), total fluorescence quenching of L_5 occurs only beyond four equivalents of Hg^{2+} indicating that the rate of quenching of fluorescence is much slower with L_5 as compared to L. Comparison of I/I_0 plots of the titration of L and L_5 (Figure 13b) with Hg^{2+} clearly differentiate the species formed in case of L_5 from that formed with L besides suggesting the binding of benzimidazole moiety to Hg^{2+}. Whereas L forms 1:1 species with Hg^{2+}, in case of L_5, at least two or three molecules are required to form the Hg^{2+} complex. All this indicates that the receptor molecule, L is more sensitive toward Hg^{2+} than the reference molecule, L_5, by using both its benzimidazole arms simultaneously wherein the calixarene moiety acts as a platform.

Comparison of the fluorescence titration data of all the reference systems with that of L clearly indicate that though the benzimidazole moiety is definitely required for binding, none of the reference compounds except L_5 is selective toward M^{2+} under the conditions studied and hence supports the role of calix[4]arene as a necessary platform and the benzimidazole moieties as binding units besides providing hydrophobic zone in the recognition of Hg^{2+}. However, L_5 has lower sensitivity toward Hg^{2+} as compared to the receptor molecule, L. Our recent study of simple diamino derivative of calix[4]arene having no benzimidazole moiety showed response to Hg^{2+} in fluorescence but does not show any selectivity, as the ion tends to go into the cavity in the absence of any preferential binding core.[9] We have also demonstrated that a binding core having chelation capability can substantially improve M^{2+} recognition at the lower rim.[10]

Fluorescence Lifetime Measurements of Mercury Binding. The fluorescence decay data of L (Figure 14a) in 50% aqueous solution can be primarily fitted to a single exponential species (98%) having lifetime of 0.45 ns that is characteristic of the benzimidazole component. Titration of this with 1 equivalent of Hg^{2+} brought significant changes in the fluorescence decay pattern that can be fitted with biexponential yielding two life times, viz., 0.55 and 0.15 ns with species ratio of 25% and 75% respectively. Further, the titration of this mixture with one additional equivalent of Hg^{2+} (a total of 2 equiv of Hg^{2+}) did not bring much change in the decay behavior by exhibiting two species with life times of 0.63 and 0.16 ns and a species ratio of 12% and 88% respectively. Thus the lifetime of the major species present in Hg^{2+} bound case results in a decrease by 3-fold. Similar trends in lifetimes were noticed between simple L_1 (Figure 14b) (0.09 ns, 93%) and {L_1 + Hg^{2+}} (0.03 ns, 100%). The difference in the lifetime of L (0.45 ns) and that of L_1 (0.09 ns) is indicative of the constricted mobility of the benzimidazole moiety when tethered to the calix[4]arene as in L. For the same reason, it is also evident from the steady state fluorescence data that while different M^{2+} quench the fluorescence in case of L_1, only Hg^{2+} quenches in case of L.

(8) (a) Wang, J.; Qian, X. *Org. Lett.* **2006**, *8*, 3721. (b) Kim, J. S.; Choi, M. G.; Song, K. C.; No, K. T.; Ahn, S.; Chang, S.-K. *Org. Lett.* **2007**, *9*, 1129.

(9) Joseph, R.; Gupta, A.; Rao, C. P. *J. Photochem. Photobiol. A* **2007**, *188*, 325.

(10) (a) Dessingou, J.; Joseph, R.; Rao, C. P. *Tetrahedron Lett.* **2005**, *46*, 7967. (b) Kumar, A.; Ali, A.; Rao, C. P. *J. Photochem. Photobiol. A* **2006**, *177*, 164.

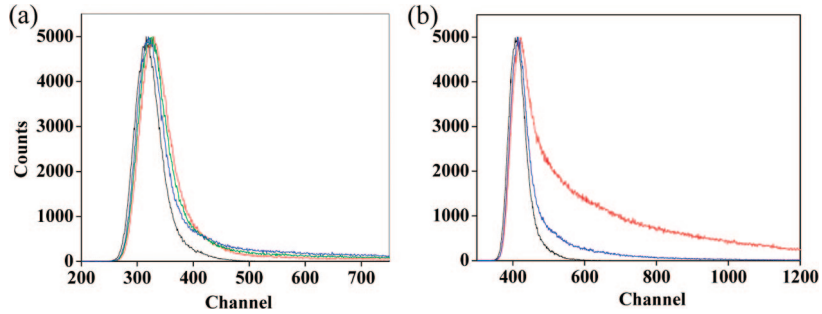

FIGURE 14. Fluorescence decay plots during the titration of Hg^{2+}: (a) in case of L, prompt (black), no Hg^{2+} but only L (red), L + 1 equiv Hg^{2+} (green), and L + 2 equiv of Hg^{2+} (blue); (b) in case of L_1, prompt (black), no Hg^{2+} but only L_1 (red), and L_1 + 2 equiv of Hg^{2+} (blue).

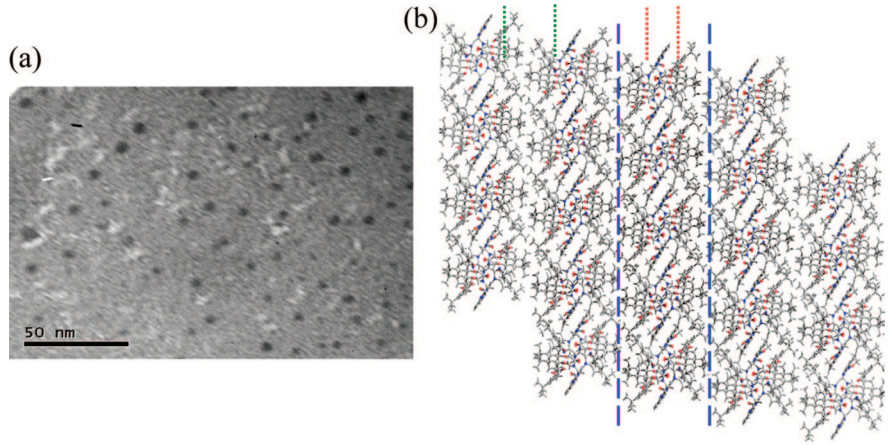

FIGURE 15. (a) TEM micrographs for the ligand L in ethanol. (b) Lattice diagram of L: hydrophobic region ~16Å (green dots), Hydrophilic region ~8 Å (red dots), and bilayer of hydrophilic and hydrophobic region ~2.4 nm (blue dashes).

Thus the fluorescence lifetime measurements clearly suggest that the Hg^{2+} ion binds to benzimidazole moieties and thereby demonstrate the advantage of these moieties when connected to the calix[4]arene platform.

To further understand the nature of the complex formed between Hg^{2+} and L, the complex has been isolated and characterized by different techniques including the study of its nanostructure in comparison with L. The Hg^{2+} binding characteristics have been further addressed based on DFT computational calculations.

Isolation and Characterization of Hg^{2+} Complex of L. From a synthetic scale reaction carried out between L and Hg^{2+}, a light-yellow product was isolated and the elemental analysis including that of Hg^{2+} suggested the formation of a complex with composition, viz., $[HgL](ClO_4)_2.4C_2H_5OH$, and was further characterized by UV−vis, ^1H NMR, and ESI MS. The ^1H NMR spectrum of this complex agrees well with that obtained during the titration of L with Hg^{2+} as reported earlier in this paper. The absorption spectrum of the complex clearly differs from that of the ligand. ESI mass spectrum exhibited molecular ion peak at 1231.77 corresponding to $[M + Hg + Li]^+$ where in the authenticity of this peak could be established based on the isotopic peak pattern indicating the presence of mercury in the molecular ion. Thus, all the characterization data supports the formation of the complex as well as the formulation satisfactorily as given in the experimental. The nanostructural behavior of this complex has been established based on different microscopy techniques, viz., transimission electron microscopy (TEM), scanning electron microscopy (SEM) and atomic force microscopy (AFM) and the results were compared with that of the ligand data.

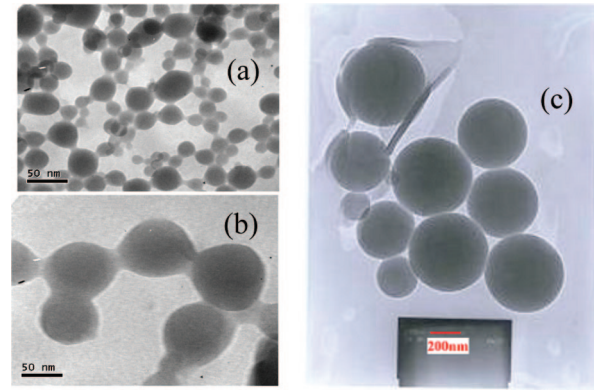

FIGURE 16. TEM micrographs for the mercury complex of L: (a) and (b) in ethanol; (c) in aqueous acetonitrile solution. Corresponding scales are shown in the figure.

Nanostructural Studies of L and Its Complex with Hg^{2+}. In TEM, the ligand (L) sample prepared from ethanol indicated the formation of reasonably uniform and well separated spherical clusters of 5−10 nm size as can be seen from the micrograph given in Figure 15a. The lattice structure of L derived based on single crystal XRD showed formation of lower rim head-to-head dimers resulting in hydrophilic core. Extension of such dimers resulted in the formation of layers of hydrophobic (16 Å) and hydrophilic (8 Å) regions where the distance between the two such adjacent layers turns out to be 2.4 nm (Figure 15b) and hence could result in the formation of nanostructures as observed in TEM.

On the other hand, in TEM the Hg^{2+} complex of L exhibit spherical clusters of sizes higher than that found for L, viz., 40−70 nm and are connected together to form chains with some

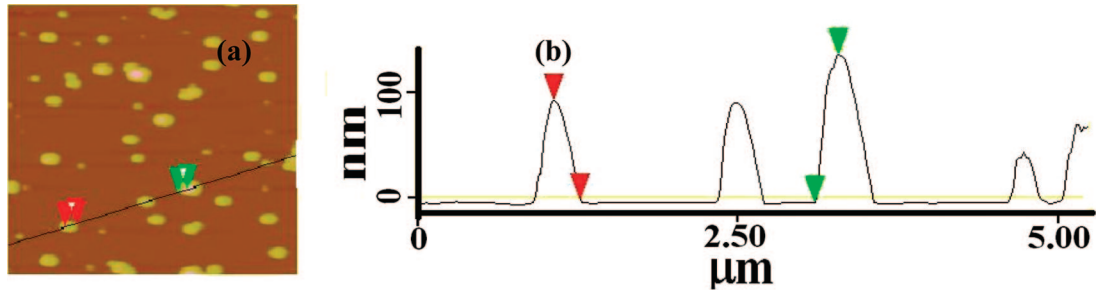

FIGURE 17. (a) Atomic force microscopy image of L in ethanol. (b) Height measurements for two particles shown in (a) with red and green markers.

branching (Figure 16a). A closer view of these chains clearly indicate that there is a reasonable overlap between the adjacent spheres so as to form a dumb-bell shaped units connected together, resulting in the distortion of the spherical nature (Figure 16b). The nanostructural behavior of mercury complex has also been found to be different from that of the simple mercury acetate studied under the same conditions. Such dumb-bell structures were reported with pyrogallol-based calix[4]arene derivative.[11] Thus the nanostructures observed in case of the Hg^{2+} complex of L in the present case may provide hinge for future studies. Since the ligand is selective toward Hg^{2+} in aqueous acetonitrile solution, TEM studies were also carried out from the samples of the mercury complex prepared from this solution. The micrographs observed in this case (Figure 16c) exhibited large size spherical nanostructures ranging from 200 to 400 nm size. A close look at these micrographs reveals that there is hardly any overlap between the spheres unlike that observed in case of the ethanol samples. This suggests that the solvent plays a role in the nanocluster formation and the self-aggregation is more in the aqueous solution system. Each of these spherical units present in the TEM micrographs of the complex may be the result of the manifestation of Hg^{2+} leading to aggregates at the molecular level formed through the connectivity of their hydrophilic mercury containing lower rim terminals and an ensemble of such units interacting through their hydrophobic upper rim terminals appropriately resulting in recognizable nanostructures in the complex.

The simple ligand in ethanol medium gives spherical particles which are well spread all over the mica sheets in AFM studies as can be noted from the micrographs given in Figure 17a. The particle height distribution can be noted from Figure 17b. The individual particle heights are found to be in the range of 90−150 nm. However, we were unable to get the AFM pictures for the mercury complex due to heavy roughness. This leads to the conclusion that in presence of Hg^{2+} the particle sizes are quite big and hence the probe-surface interaction is high enough to give large roughness.

The ligand shows high crystallinity in scanning electron micrographs whereas the mercury complex does not show any crystalline nature (Figure 18). The noncrystalline nature of the mercury complex has also been evidenced from electron diffraction of a particle in TEM studies.

It can be noted from the X-ray diffractogram that the ligand L (Figure 19) is highly crystalline, as can also be understood from the single crystal structure reported in this paper. However, the powder diffractogram of the mercury complex of L showed a broad hump in the 2θ region of 10−40° indicating that the mercury complex is noncrystalline.

Thus, the TEM clearly indicated that there exists a difference in the nanostructure formed by L when compared to its Hg^{2+} complex. The noncrystalline nature of the mercury complex of L has been delineated based on microscopy as well as the diffraction data, and thus, the microscopy studies seem to be useful in differentiating the complex from that of the ligand.

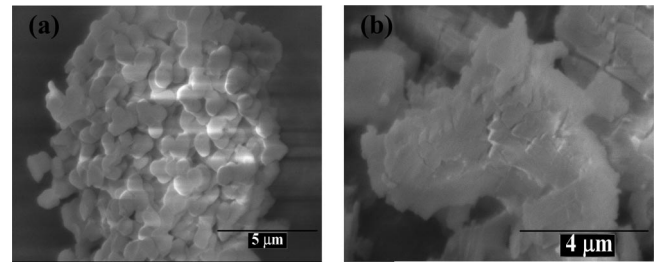

FIGURE 18. SEM micrographs: (a) L and (b) mercury complex of L.

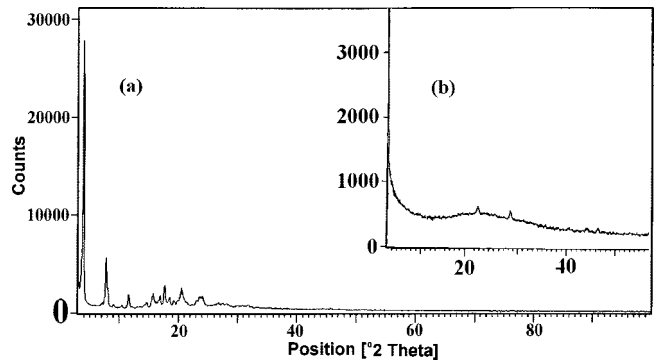

FIGURE 19. Powder X-ray diffractograms: (a) for the ligand, L and (b) for the mercury complex of L.

Because there was no crystal structure of the Hg^{2+} complex available, the complexation was modeled by density functional theory (DFT) based computational studies.

Computational Optimization of the Hg^{2+} Complex of L. All the computational calculations reported here were performed using Gaussian 03 package.[12] The crystal structure of the ligand L has been taken as the initial guess and was optimized to highest level of HF/6−31G through a cascade process, viz., AM1 → HF/STO-3G → HF/3−21G → HF/6−31G. The initial guess for the mercury complex was obtained by taking the optimized structure of L from HF/6−31G and simply placing the Hg^{2+} ion well above the binding core so that there are no interactions present between Hg^{2+} and L. This initial guess structure for the mercury complex was optimized using DFT

(11) Heaven, M. W.; Cave, G. W. V.; McKinlay, R. M.; Antesberger, J.; Dalgarno, S. J.; Thallapally, P. K.; Atwood, J. L. *Angew. Chem., Int. Ed.* **2006**, *45*, 6221.

(12) Frisch, M. J. *Gaussian 03*, revision C.02; Gaussian, Inc.: Wallingford, CT, 2004. The full reference is listed in the Supporting Information S8.

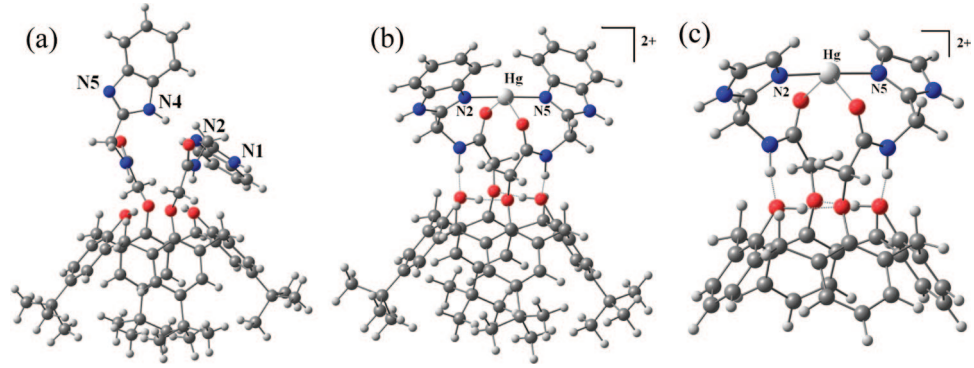

FIGURE 20. (a) Crystal structure of L being optimized in HF/6−31G. (b) B3LYP/CEP-121G optimized structure of the $[HgL]^{2+}$ (c) B3LYP/CEP-121G optimized structure of the $[HgL']^{2+}$. The large gray sphere is mercury ion.

TABLE 3. Dihedral Angles of Both the Arms of the Structures Optimized by B3LYP/CEP−121G[a]

dihedral angle	L		Hg−L		L′		Hg−L′	
D1	131.2	118.4	141.3	141.3	131.9	126.6	141.0	140.9
D2	−1.9	17.6	−29.3	−29.4	−4.6	4.5	−26.6	−26.5
D3	−174.6	−178.4	−153.1	−153.1	−177.3	179.0	−153.1	−153.1
D4	−123.4	−126.7	−101.3	−101.2	−128.7	−127.1	−102.3	−102.1

[a] Dihedral angles D1−D4 have the same meaning as in Table 2.

computations (Supporting Information, S7) by going through B3LYP/CEP-31G followed by B3LYP/CEP-121G.[13] The optimization study resulted in the formation of a linearly coordinated species of the type N2···Hg···N5 (178.6°) with Hg···N distance of 2.092 Å (Figure 20a). Such linear coordination was proposed in case of a tetra-4-picolyl derivative of calix[4]arene in the literature.[14] In addition the structure also reveals weak interaction with the amide carbonyl oxygens where the Hg···O distance was found to be 2.7 Å. Weak interactions present between the Hg^{2+} and oxygen have been reported in the literature.[15] Comparison of the benzimidazole arms in L (Figure 20a) with those present in the complex (Figure 20b) suggests that the corresponding dihedral angles have to be changed to bring N_2 and N_5 in line to form coordination with Hg^{2+} when compared to that present in the free ligand (Table 3). As the computational times involved with L was enormously high, initial calculations were performed using mutilated ligand, L′ wherein the L′ was generated from L simply by replacing the tertiary butyl groups and the benzene portion of the benzimidazole by hydrogens. Thus the computational optimizations were also done with $[HgL]^{2+}$ as well as with $[HgL']^{2+}$. In both the ligands, viz., L and L′, the conformations of the arms were found to be similar (Table 3). Also the geometry about the Hg^{2+} was found to be exactly same in both the complexes, viz., $[HgL]^{2+}$ and $[HgL']^{2+}$ (Figure 20).

The stabilization energies were computed using the formula, $\Delta E_s = \Delta E_{complex} - (\Delta E_{lig} + \Delta E_{M^{2+}})$. On the basis of these calculations, gas phase stabilization energies were found to be −355.2 and −393.9 Kcal/mol, respectively, for the complexes $[HgL]^{2+}$ and $[HgL']^{2+}$. Single point energy of these optimized complexes were computed in presence of acetonitrile and water solvent dielectric fields and the corresponding average stabilization energies were computed to be −187.9 and −291.7 kcal/mol for $[HgL]^{2+}$ and $[HgL']^{2+}$, respectively.

Conclusions

Selective recognition of Hg^{2+} by calix[4]arene derivative has been addressed by us in this paper both from the point view of organic fine-tuning of the lower rim arm derivatization as well as to understand its capacity in recognizing Hg^{2+} even in the presence of other M^{2+}. To achieve this goal, identification of the species of recognition is of utmost importance both in solution phase and also in its isolated form. In effect the studies related to these are being addressed in this paper both by experimental as well as by computational approaches. Synthetic modification in the arms at the lower rim resulted in different derivatives which can be used as reference compounds. The reference compounds were chosen in such a way that there is a similarity between these molecules and receptor molecule only in one feature at a time and there is a smooth change in the features of one reference molecule to the other.

Thus, the receptor L has been shown to be sensitive (1.4 ± 0.1 ppm) and selective to Hg^{2+} among 11 divalent metal ions studied as well as 5 different reference compounds compared with, and further found that aqueous acetonitrile was best suited solvent combination for sensing Hg^{2+} by L through the formation a 1:1 complex. Even the other ions from the same group, viz., Zn^{2+} and Cd^{2+}, do not bind to L. None of the M^{2+} impedes the interaction of Hg^{2+} with L. Thus L is very sensitive and selective toward Hg^{2+} even in the presence of other M^{2+} ions. All the data obtained based on L, comparison of this with that obtained for L_1 to L_5, suggested the necessity of the calix[4]arene platform, benzimidazole binding core as well as the presence of hydrophobic moiety in the vicinity of the binding core for the recognition of Hg^{2+}. Examination of the crystal structures of the receptor molecule, viz., L, with those of the reference molecules, viz., L_2, L_3, L_4, and L_5, clearly demonstrated the advantage of the benzimidazole moiety in forming a binding core that would easily respond to the metal ion

(13) Jian, F. F.; Zhao, P. S.; Ma, H. B. *Struct. Chem.* **2005**, *16*, 469.
(14) de Namor, A. F. D.; Cornejo, A. A.; Sonalhi, R.; Shehab, M.; Nolan, K. B.; Ouazzani, N.; Mandi, L. *J. Phys. Chem. B* **2005**, *109*, 14735.
(15) (a) Hossain, G. M. G.; Amoroso, A. J.; Banu, A.; Malik, K. M. A. *Polyhedron* **2007**, *26*, 967. (b) Lourenco, L.; Marques, L. L.; Lang, E. S.; Fennera, H.; Castellano, E. E. *Z. Anorg. Allg. Chem* **2005**, *631*, 745. (c) Meyer, G. Nockemann, Peter. *Z. Anorg. Allg. Chem.* **2003**, *629*, 1447. (d) Garcia-Raso, A.; Fiol, J. J.; Rigo, S.; Lopez-Lopez, A.; Molins, E.; Espinosa, E.; Borras, E.; Alzuet, G.; Borras, J.; Castineiras, A. *Polyhedron* **2000**, *19*, 991.

presence. The observed difference in the sensitivity and selectivity toward Hg^{2+} by L and L_3, the two closely related derivatives, may be addressed owing to the presence of two nitrogen centers per arm in the former while it is only one nitrogen center in the latter besides the difference in their coordinating ability of their nitrogen centers. This has provided additional advantage for L to sense as well as to select metal ion better than the L_3 and also better than the other reference molecules. Though L_5 is also sensitive toward Hg^{2+}, it requires higher equivalents of Hg^{2+} for quenching the fluorescence of L_5 as compared that required for L and hence L is more sensitive toward Hg^{2+} than the reference molecule, L_5.

Thus the present study clearly provided a molecular design approach for calix[4]arenes for their sensing toward Hg^{2+}. The complex species formed between L and Hg^{2+} has been further proven in solution by absorption, NMR, ES MS and fluorescence lifetime measurements. To further understand the nature of the complex formed between Hg^{2+} and L, the complex has been isolated and characterized and its composition has been established to be 1:1 complex. Transmission electron microscopy indicated that there exists a clear-cut difference in the nanostructure formed by L when compared to its Hg^{2+} complex indicating that the TEM can provide a means to differentiate L from its mercury complex. Both the SEM and powder XRD studies demonstrated the crystallinity difference between the L and its mercury complex, wherein the mercury complex is amorphous, perhaps a reason for us not been able to obtain single crystals of the mercury complex. Detailed studies of microscopy of such receptor systems and their metal ion complexes are currently underway in our laboratory. The structure of the mercury complex has been further demonstrated based on DFT computational calculations performed with B3LYP/CEP-121G using $[HgL]^{2+}$ and $[HgL']^{2+}$.

Experimental Section

All the perchlorate salts were procured from Sigma Aldrich Chemical Co., U.S.A. All the solvents used were dried and distilled by usual procedures immediately before use. Distilled and deionized water was used in the studies. ^1H and ^{13}C NMR spectra were measured on a Varian Mercury NMR spectrometer working at 400 MHz. The mass spectra were recorded on Q-TOF micromass (YA-105) using electrospray ionization method. The time-resolved single photon counting (TCSPC) was measured on fluorocube time-resolved fluorescence spectrometer from IBH, UK. Steady state fluorescence spectra were measured on Perkin-Elmer LS55. The absorption spectra were measured on Shimadzu UV2101 PC. The elemental analyses were performed on ThermoQuest microanalysis. FT IR spectra were measured on Perkin-Elmer spectrometer using KBr pellets. Single crystal X-ray diffraction data were measured on OXFORD XCALIBUR-S CCD machine. TEM experiments were performed on a JEOL 1200 EX transmission electron microscope operating at 80−120kV. AFM studies were performed in multimode Veeco Dimensions 3100 SPM with Nanoscope IV controller instrument. SEM was performed on a Hitachi S3400 cold-cathode Field Emission Scanning Electron Microscope (Hitachi High Technologies America, Inc., Pleasanton, CA). All the computational calculations were performed using Gaussian 03 package.

Synthesis and Characterization Data for the Receptor Molecule L. 1. The p-tert-butyl-calix[4]arene, **1**, is synthesized by the condensation of *p*-tert-butyl-phenol with formaldehyde in presence of NaOH as per the procedure given by Gutsche and coworkers (ref: *J. Am. Chem. Soc.*, **1981**, *103*, 3782).

2. A mixture of **1** (10 g, 15.4 mmol), potassium carbonate (4.26 g, 30.8 mmol), and ethyl bromoacetate (5.14 mL, 30.8 mmol) were taken in dry acetone (1.6 L) and stirred and heated at reflux for 15 h under nitrogen atmosphere. The cooled reaction mixture was filtered through a bed of celite and the filtrate and dichloromethane washings of the celite were combined and concentrated to dryness. Recrystallization of the residue from ethanol yielded the diester. Yield (9.86 g, 78%). ^1H NMR ($CDCl_3$, δ ppm): 0.98 (s, 18H, $C(CH_3)_3$), 1.26 (s, 18H each, $C(CH_3)_3$), 1.34 (t, 6H, CH_2-CH_3, J = 7.02 Hz), 3.32 (d, 4H, Ar−CH_2−Ar, J = 13.4 Hz), 4.30 (q, 4H, CH_2-CH_3), 4.45 (d, 4H, Ar−CH_2−Ar, J = 13.2 Hz), 4.73 (s, 4H, OCH_2CO), 6.82 (s, 4H, Ar−**H**), 7.02 (s, 4H, Ar−**H**), 7.06 (s, 2H, O**H**).

3. A mixture of the diester, **2**, (10 g, 12.2 mmol) and 15% aq. sodium hydroxide (32 mL) in ethanol (500 mL) was stirred and heated under reflux for 24 h and the reaction mixture was evaporated under reduced pressure to yield a white residue. The residue was diluted (suspension) with cold water (500 mL), and hydrochloric acid (3 N) was added with vigorous mixing until pH 1 was reached. The solid was filtered, dried in air, and further dissolved in chloroform. The solution was washed with hydrochloric acid (3 N) and brine, dried, and concentrated to afford the diacid product, **3**. **3** was recrystallized from aq. acetone (acetone:water, 7:3 v/v). Yield (7.92 g, 85%). ^1H NMR ($CDCl_3$, δ ppm): 1.10 (s, 18H each, $C(CH_3)_3$), 1.30 (s, 18H each, $C(CH_3)_3$), 3.46 (d, 4H, Ar−CH_2−Ar, J = 13.74 Hz), 4.13 (d, 4H, Ar−CH_2−Ar, J = 13.44 Hz), 4.70 (s, 4H, OCH_2CO), 6.99 (s, 4H, Ar−**H**), 7.07 (s, 4H, Ar−**H**).

4. To dry benzene (100 mL), *p*-tert-butylcalix[4]arene diacid, 3, (4.0 g) and $SOCl_2$ (6 mL) were added and refluxed under nitrogen atmosphere for 4 h. The solvent and residual $SOCl_2$ were removed under reduced pressure, and this yielded diacid chloride 3 as off white solid and was used *in situ* for the preparation of L.

5,11,17,23-Tetra-tert-butyl-25,27-bis((2-aminomethylbenzimidazole)carbonylmethoxy)-26,28-dihydroxycalix[4]arene, L. A suspension of 2-(aminomethyl)benzimidazole. 2HCl (2.73 g, 12.4 mmol) and Et_3N (6 mL, 43.1 mmol) was stirred in dry THF (100 mL) under argon atmosphere. Diacid chloride, **4** (4.32 g, 5.34 mmol) in dry THF (50 mL) was added dropwise to this reaction mixture. Immediately, a yellowish precipitate was formed and stirring was continued for 48hrs at room temperature. After filtration, the filtrate was concentrated to dryness. A yellow solid was obtained which was extracted with $CHCl_3$, washed with water and then with brine and the organic layer was dried with anhydrous $MgSO_4$. Filtrate was concentrated to dryness and recrystallized from EtOH/$CHCl_3$ to get **L** as a white solid. Yield (55%, 2.95 g) $C_{64}H_{74}N_6O_6$ (1023.29): Anal. (% found) C 67.58, H 7.50, N 6.76, $C_{64}H_{74}N_6O_6.2C_2H_5OH.CHCl_3$ (% requires) C 67.11, H 7.11, N 6.80). FTIR: (KBr, cm^{-1}): 1679 $\nu_{C=O}$), 3380 ν_{OH}). ^1H NMR: ($CDCl_3$, δ ppm): 0.98 (s, 18H, $(C(CH_3)_3)$, 1.25 (s, 18H, $(C(CH_3)_3)$, 3.28 (d, 4H, Ar−CH_2−Ar, J = 13.30 Hz), 3.96 (d, 4H, Ar−CH_2−Ar, J = 13.30 Hz), 4.40 (s, 4H, −CH_2CONH−), 4.88 (d, 4H, −CONHCH_2−, J = 5.50 Hz), 6.8 (s, 4H, Ar-**H**), 7.03 (s, 4H, Ar−**H**), 7.23−7.25 (m, 4**H**, benzimidazole), 7.53−7.55 (m, 4**H**, benzimidazole), 7.45 (s, 2H, −O**H**), 8.95 (t, 2H, −N**H**, J = 5.19). ^{13}C NMR: ($CDCl_3$, 400 MHz δ ppm): 31.10, 31.8 ($C(\boldsymbol{C}H_3)_3$), 32.1(Ar−$\boldsymbol{C}H_2$−Ar), 34.0, 34.2 ($\boldsymbol{C}(CH_3)_3$), 37.3 ($\boldsymbol{C}H_2$−benzimidazole), 73.8 ($O\boldsymbol{C}H_2CO$), 114.9, 124.1, 125.5, 126.1, 127.4, 135.5, 135.9, 142.7, 148.1, 149.2, 149.8, 152.0, (benzimidazole and calix-Ar-**C**), 170.6 (***C***=O). *m/z* (ES-MS) 1023.72 ($[M]^+$ 100%), 1024.7 ($[M+H]^+$ 35%,). Single crystals of L were obtained by slow evaporation of the solvent mixture (EtOH/$CHCl_3$) at room temperature to give single crystals of L.

Synthesis and Characterization Data for the Reference Compounds, L_1, L_2, L_3, L_4, and L_5. L_1. 2-Aminomethylbenzimidazole, L_1 is being procured as 2HCl salt from Sigma Aldrich Chemical Co. and was used in the reactions. The fluorescence studies of this molecule in presence of M^{2+} were carried out upon neutralizing the HCl salt by using Et_3N.

L_2. A suspension of dibenzylamine (2.55 g, 12.4 mmol) and Et_3N (3 mL, 21.57 mmol) was stirred in dry THF (100 mL) under argon atmosphere. Diacid chloride, **3** (4.32 g, 5.34 mmol) in dry THF (50 mL) was added dropwise to this reaction mixture. Immediately a yellowish precipitate was formed and stirring was continued for

48 h at room temperature. After filtration, the filtrate was concentrated to dryness. A yellow solid was obtained, which was extracted with $CHCl_3$ and washed with water and then with brine, and the organic layer was dried with anhydrous $MgSO_4$. Filtrate was concentrated to dryness and recrystallized from EtOH/$CHCl_3$ to get **L_2** as white crystalline solid. Yield (3.5 g, 60%.). $C_{76}H_{86}N_2O_6 \cdot CHCl_3$ (1242): Anal. (% found) C 74.90, H 7.59, N 2.36, (% requires) C 74.43, H 7.01, N 2.26. FTIR: (KBr, cm^{-1}): 1667 ($\nu_{C=O}$), 3371 (ν_{OH}). ^{1}H NMR: ($CDCl_3$, δ ppm): 0.97 (s, 18H, (C(C**H**$_3$)$_3$), 1.26 (s, 18H, (C(C**H**$_3$)$_3$), 3.26 (d, 4H, Ar−C**H**$_2$−Ar, J = 13.30 Hz), 4.37 (d, 4H, Ar−C**H**$_2$−Ar, J = 13.30 Hz), 4.60, 4.70 (s, 4H, N−C**H**$_2$) 4.82 (s, 4H, −OC**H**$_2$CO), 6.87 (s, 4H, Ar-**H**), 7.00 (s, 4H, Ar−**H**), 7.24 (s, 2H, −O**H**), 7.31 (m, 10H, benzyl-H).. ^{13}C NMR: ($CDCl_3$, δ ppm): 31.2, 31.8 (C(***C***H$_3$)$_3$), 32.0(Ar−***C***H$_2$−Ar), 33.9, 34.0 (***C***(CH$_3$)$_3$), 49.4, 48.6 (−N***C***H$_2$), 74.1 (O***C***H$_2$CO), 125.1, 125.8, 126.8, 127.4, 127.7, 127.9, 128.7, 129.1, 133.0, 136.5, 137.0, 141.3, 147.2, 150.7, 151.16 (Ar−**C**), 168.8 (***C***═O). ES-MS: *m/z* (intensity (%), fragment) 1146.53 (40, $[M + Na]^+$). ^{1}H and ^{13}C NMR spectra are given in the Supporting Information, Figure S9.

L_3. This compound was synthesized by following the procedure given for L except using 2-(aminomethyl)pyridine (1.40 g, 12.94mmol), Et_3N (2.18 g, 21.57mmol), and diacid chloride (4.32 g, 5.34 mmol), in dry THF (150 mL). The crude product was recrystallized by slow evaporation of the solvent from C_2H_5OH/$CHCl_3$. Yield (2.69 g, 52%.) FTIR: (KBr, cm^{-1}): 1682 ($\nu_{C=O}$), 3338 (ν_{OH}). ^{1}H NMR: ($CDCl_3$, δ ppm): 0.91 (s, 18H, (C(C**H**$_3$)$_3$), 1.20 (s, 18H, (C(C**H**$_3$)$_3$), 3.28 (d, 4H, Ar−C**H**$_2$−Ar, J = 13.48 Hz), 3.98 (d, 4H, Ar−C**H**$_2$−Ar, J = 13.48 Hz), 4.45 (s, 4H, −OC**H**$_2$), 4.61 (d, 4H, −NH−C**H**$_2$, J = 5.15 Hz), 6.76 (s, 4H, Ar−**H**), 6.96 (s, 4H, Ar−**H**), 7.07 (t, 2H, Py−**H**, J = 6.10 Hz), 7.14 (s, 2H, −O**H**), 7.32 (d, 2H, Py−**H**, J = 7.53 Hz), 7.56 (t, 2H, Py−**H**, J = 7.73 Hz), 8.31 (d, 2H, Py−**H**, J = 4.76 Hz), 9.10 (t, 2H, N**H**CO, J = 5.15 Hz) ^{13}C NMR: ($CDCl_3$, δ ppm): 31.1, 31.7 (C(***C***H$_3$)$_3$), 32.1(Ar−***C***H$_2$−Ar), 34.0, 34.2 (***C***(CH$_3$)$_3$), 45.4 (−N***C***H$_2$), 74.9 (O***C***H$_2$CO), 122.4, 122.4, 125.6, 126.2, 127.2, 132.2, 136.7, 142.9, 148.3, 149.2, 149.4, 149.7, 156.9 (Ar−**C**), 168.62 (***C***═O). ESI-MS: *m/z* (intensity (%), fragment) 946.6 (30, $[M + 1]^+$).

L_4. In 50 mL of THF solution of **3** (1.0 g, 1.3 mmol), 1-hydroxybenztriazol (0.392 g, 2.9 mmol) and DCC (0.598 g, 2.9 mmol) were stirred at room tempreture. To this, L-phenylalanine methyl ester hydrochloride (0.625 g, 2.9 mmol) and triethyl amine (1.5 mL) in 30 mL THF were added dropwise. Stirring was continued for 48 h. Solvent was evaporated under reduced pressure. The solid was redissolved in CH_2Cl_2. The reaction mixture was washed with 1 N HCl followed by brine and the organic layer was collected and dried with anhydrous Na_2SO_4. After filtration, the solvent was removed under reduced pressure. The pure product was obtained as white powder (0.75 g, 56.0%). $C_{68}H_{82}N_2O_{10} \cdot$ (1086): Anal. (% found) C 74.75, H 7.20, N 2.75, (% requires) C 75.14, H 7.55, N 2.58. FTIR (KBr, cm^{-1}): 3458, 3304 ($\nu_{NH/OH}$), 1752 ($\nu_{C=O}$, COOMe), 1670 ($\nu_{C=O}$, CONH). ^{1}H NMR ($CDCl_3$, δ ppm): 1.02, 1.30 (s, 36H, C(C**H**$_3$)$_3$), 3.02−3.15 (m, 6H, Ar−C**H**$_2$−Ar, and C$^{\beta}$**H**$_2$−Ph), 3.47 (d, 2H, Ar−C**H**$_2$−Ar, J = 13.76 Hz), 3.64 (s, 6H, OC**H**$_3$), 4.06 (d, 2H, Ar−C**H**$_2$−Ar, J = 12.9 Hz), 4.10 (d, 2H, Ar−C**H**$_2$−Ar, J = 14.2 Hz), 4.14 (d, 2H, O−C**H**$_2$−CO, J = 15.2 Hz), 5.03 (d, 2H, O−C**H**$_2$−CO, J = 15.0 Hz), 5.10 (q, 2H, C$^{\alpha}$**H**, J = 7.8, 7.0 Hz), 6.87 (d, 4H, Ar−**H**), 7.03 (m, 14H, Ar−**H**, Ph−**H**), 7.73 (s, 2H, O**H**), 9.51 (d, 2H, N**H**, J = 8.3). ^{13}C NMR ($CDCl_3$, 400 MHz,): δ 30.9, 31.7 (C(***C***H$_3$)$_3$), 32.0, 32.5 (Ar−***C***H$_2$−Ar), 33.9, 34.0 (tert-***C***), 39.0 (***C***H$_2$−Ph), 52.1 (O***C***H$_3$), 52.8 (***C***H), 74.9 (O-***C***H$_2$−CO), 124.7, 125.3, 125.8, 126.4, 126.5, 126.7, 127.6, 128.1, 128.9, 132.6, 136.1, 142.3, 147.8, 149.7, 150.0 (aromatic carbons), 168.8 (***C***ONH), 171.8 (***C***OOMe) ppm. ES-MS: *m/z* = 1087 ($[M + H]^+$, 100%). ^{1}H and ^{13}C NMR spectra are given in Supporting Information, Figure S9.

L_5. Reference compound L_5 has been synthesized as shown in Scheme 2. ^{1}H and ^{13}C NMR spectra are given in the Supporting Information, Figure S9.

SCHEME 2. Synthesis of L_5[a]

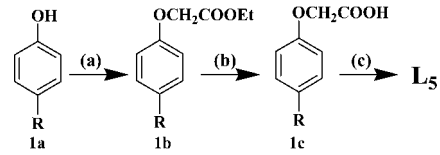

[a] (a) bromoethylacetate/K_2CO_3/ acetone; (b) KOH/C_2H_5OH/Water, reflux; (c) EDCI/ Et_3N/ HOBT/2-aminomethyl benzimidazole. R = tert-butyl.

1b: A mixture of *p-tert*-butyl phenol, **1a** (2.00 g, 13.3 mmol), potassium carbonate (2.40 g, 17.3 mmol), and ethyl bromoacetate (1.77 mL, 15.99 mmol) was taken in dry acetone (150 mL), and the reaction mixture was stirred and heated at reflux for 12 h under nitrogen atmosphere. The cooled reaction mixture was concentrated under reduced pressure. The residue was dissolved in $CHCl_3$ and washed with 1N HCl. The organic layer was separated and washed with brine followed by drying using $MgSO_4$. After filtration, solvent was evaporated by drying under vacuum to result in a yellow oil. Yield (3.20 g, 97%). ^{1}H NMR ($CDCl_3$, δ ppm): 1.29 (s, 9H, C(C**H**$_3$)$_3$), 1.30 (t, 3H, CH$_2$(C**H**$_3$)$_3$), 4.28 (q, 2H, C**H**$_2$−CH$_3$, J = 7.33 Hz), 4.59 (s, 2H, OC**H**$_2$CO), 6.84 (d, 2H, Ar−**H**, J = 8.86 Hz), 7.30 (d, 2H, Ar−**H**, J = 8.85 Hz).

1c: A mixture of the **1b**, (3.20 g, 13.55 mmol) and potassium hydroxide (1.6 g, 28.46mmol) in 120 mL of ethanol:water (2:1 v/v) mixture were stirred and heated under reflux for 12 h and the reaction mixture was evaporated under reduced pressure to yield a white residue. The residue was taken in 1 N HCl (100 mL) and $CHCl_3$ (250 mL). The organic layer was washed with water and dried over $MgSO_4$. All the organic solvent was evaporated to yield white solid as pure product. Yield (2.00 g, 71%). ^{1}H NMR ($CDCl_3$, δ ppm): 1.29 (s, 9H each, C(C**H**$_3$)$_3$), 4.66 (s, 2H, OC**H**$_2$CO), 6.86 (d, 2H, Ar−**H**, J = 8.86 Hz), 7.32 (d, 2H, Ar−**H**, J = 8.85 Hz).

L_5: To a solution of **1c** (0.3 g, 1.44mmol) in CH_2Cl_2 (75 mL) was added Et_3N (1.00 mL, 7.21mmol), 1-ethyl-(3-dimethylaminopropyl)-3-carbodiimide hydrochloride (EDCI.HCl) (0.41 g, 2.16mmol) and catalytic amount of 1-hydroxybenzotriazole (HOBT) and stirred the solution at 0 °C for 30 min under N_2 atmosphere. 2-Aminomethyl benzimidazole (0.48 g, 2.16mmol) was added to this reaction mixture and stirred at room temperature for overnight. The resulting mixture was washed with water followed by saturated $NaHCO_3$ and brine. The product can be purified either by using silica gel column with chloroform-methanol as eluant or alternatively by dissolving the impurities in dichloromethane and filtering off the product, to give white solid. Yield (0.36 g, 74%). $C_{20}H_{23}N_3O_2.CH_3OH \cdot$ (369.45): Anal. (% found) C 67.82, H 7.10, N 10.94, (% requires) C 68.27, H 7.36, N 11.37. FTIR: (KBr, cm^{-1}): 1654 ($\nu_{C=O}$). ^{1}H NMR (DMSO-d_6, δ ppm): 1.24 (s, 9H, C(C**H**$_3$)$_3$), 4.56 (s, 2H, OC**H**$_2$), 4.58 (s, 2H, NC**H**$_2$), 6.92 (d, 2H, Ar-**H**, J = 8.86 Hz), 7.14 (m, 2H, Benz-**H**), 7.30 (d, 2H, Ar-**H**, J = 8.86 H), 7.51 (br, 2H, Benz-**H**), 8.78 (t, 1H, CON**H**, J = 5.80 Hz), 12.31 (s, 1H, Benz-N**H**). ^{13}C NMR: (DMSO-d_6, δ ppm): 31.4, 33.8, 36.9, 67.0, 79.3, 114.3, 121.4, 126.1, 143.4, 152.1, 155.6, 168.4. ESI MS: *m/z* (intensity (%), fragment) 338.3 (100, $[M + H]^+$).

Synthesis, Isolation, and Characterization of the Hg^{2+} Complex of L. Metal salt, $Hg(ClO_4)_2$ (0.094 g, 0.235 mmols) was dissolved in CH_3OH (5 mL) and was added to the ligand, L (0.20 g, 0.196 mmols) in $CHCl_3$. The solution was stirred overnight followed by refluxing for 12 h. The resulting solution was concentrated, washed with minimum amount of methanol and dried under vacuum. Yield (80%, 0.22 g). ^{1}H NMR: ($CDCl_3$, 400 MHz δ ppm): 1.10 (s, 18H, (C(C**H**$_3$)$_3$), 1.14 (s, 18H, (C(C**H**$_3$)$_3$), 3.43 (d, 4H, Ar−C**H**$_2$−Ar, J = 12.50 Hz), 4.10 (d, 4H, Ar−C**H**$_2$−Ar, J = 12.50 Hz), 4.65 (s, 4H, −C**H**$_2$CONH−), 5.33 (s, 4H, −CONHC**H**$_2$−), 7.10 (s, 4H, Ar−**H**), 7.13 (s, 4H, Ar−**H**), 7.52 (m, 4**H**, benzimidazole), 7.76 (s, 2**H**, benzimidazole), 8.19 (s, 2H, −O**H**), 8.27 (m, 2H, benzimidazole), 9.75 (s, 2H, CON**H**), 14.56 (s, 2H, −N**H**-benzimidazole). Anal. (% found) C 53.02, H 6.41, N 5.57, Hg 12.92. $C_{64}H_{74}N_6O_6.4C_2H_5OH.Hg(ClO_4)_2$ (% required) C 53.41,

H 6.10, N 5.21, Hg 12.49. ES MS 1231.77 ([M + Hg + Li]$^+$) UV−vis spectral data λ, nm (ε, mole.lit^{-1}.cm^{-1}): 263 (13932); 270 (18314); 277 (17753); 292 (5168).

Details of Solution Studies. All the metal salts used for the titrations were as their perchlorate salts (Caution: perchlorate salts may explode under some conditions) with a formula, $M(ClO_4)_2.xH_2O$. All the solvents used were of analytical grade and were purified and dried by routine procedures immediately before use.

Fluorescence Studies. Fluorescence emission spectra were measured on Perkin-Elmer LS55 by exciting the solutions at 275 nm and the emission spectra were recorded in the 285−400 nm range. Different solvent or solvent combinations were used for fluorescence studies are CH_3OH, CH_3CN, H_2O:CH_3CN (1:1), H_2O:CH_3CN (1:3), and H_2O:CH_3CN (3:2). The fluorescence studies performed in CH_3OH solution uses always a 50 μL of chloroform solution of L (i.e., the 3 mL solution contains 2.950 mL of CH_3OH and 0.050 mL of $CHCl_3$). All the measurements were made in 1 cm quartz cell and maintained a final L concentration of 10 μM. During the titration, the concentration of metal perchlorate was varied accordingly to result in requisite mole ratios of metal ion to L and the total volume of the solution was maintained constant at 3 mL in each case by adding appropriate solvent or solvent mixtures. Normalized emission (relative fluorescence) intensities (I/I_0) (where, I_0 is the intensity with no metal ion addition; I is the intensity at different metal ion to L mole ratios) were plotted against the mole ratio of metal ion to the L. The association constant of the mercury complex formed in the solution has been estimated using the standard Benesi-Hildebrand equation, viz.,

$$\frac{1}{I-I_0} = \frac{1}{I_1-I_0} + \frac{1}{(I_1-I_0)K_a[M^{2+}]} \qquad (1)$$

where I_0 is the intensity of L, I is the intensity in the presence of M^{2+}, I_1 is intensity upon saturation with M^{2+} and K_a is the association constant of the complex formed.

The same procedure was followed in the case of the M^{2+} titration of L_2. Whereas in the case of L_1, the hydrochloride salt of L_1 was first dissolved in water and neutralized with Et_3N prior to the titration.

Absorption Studies. L (0.00303 M) was dissolved in CH_3CN, and $Hg(ClO_4)_2$ (0.00303 M) taken in H_2O:CH_3CN (1:1) were used for titrations. Titrations were carried out by varying the equivalents of metal ion between 0 and 4.0 using the additions of 0, 20, 40, 60, 80, 100, 120, 160, 180, 220, 250, 300, 350, and 400 μL stock solution and by fixing the ligand concentration as constant at 100 μL and all the solutions were diluted to 3 mL using H_2O:CH_3CN (1:1) solvent system before used for the study. Same procedure was followed for recording the absorption spectra of the titration of metal ions Zn^{2+} and Cd^{2+} with L.

NMR Titration Experiments. (a) Hg^{2+} titration with L. L (0.0245 M) was dissolved in 0.4 mL of DMSO-d_6 and recorded the ^{1}H NMR spectra. Metal ion titrations were carried out by adding different volumes of, viz., 10, 20, 30, 40, 60, 80, 120, and 160 μL of bulk $Hg(ClO4)_2$ (0.245 M) solution to a solution of L to result in $[Hg^{2+}]/[L]$ mole ratio of 0−4 (b) Zn^{2+} titration with L. Same procedure as in (a) was followed in the titration of Zn^{2+} with L.

Microscopy Studies. TEM experiments were performed on a JEOL 1200 EX transmission electron microscope operating at 80−120kV. Carbon coated copper grids of 300 mesh were used as substrate for the sample. Stock solutions of the samples were prepared by dispersing the weighed sample in appropriate solvent followed by sonicating the mixture for 30 min to result in a concentration of $\sim 6 \times 10^{-4}$ M. Different sample blocks were made by placing 5−10 μL of the sample solution on the copper grid and allowing it to dry in air at room temperature. AFM studies were performed in multimode Veeco Dimensions 3100 SPM with Nanoscope IV controller instrument. Contact mode with non conductive silicon nitride probe having sharp fine tip at the end was used in all the cases. Sample preparation was identical with TEM sample preparation. Mica sheets were used as substrate for the studies. SEM was performed on a Hitachi S3400 cold-cathode Field Emission Scanning Electron Microscope (Hitachi High Technologies America, Inc., Pleasanton, CA). SEM experiment grids were prepared by gold coating.

Acknowledgment. C.P.R. acknowledges the financial support by DST, CSIR, and BRNS-DAE. R.J. thanks UGC and A.A. thanks CSIR for their research fellowships. We thank Dr. M. Dey and Dr. P. Guionneau for providing the XRD data for L_2.

Supporting Information Available: Single crystal X-ray structural information (Figure S1), fluorescence titration data (Figures S2−S4), NMR titration data (Figures S5 and S6), computational data (Figure S7), full reference of Gaussian 03 (Figure S8), and NMR spectra for L_2 and L_4, L_5 (Figure S9). This material is available free of charge via the Internet at http://pubs.acs.org.

JO800073G